Journal of Volcanology and Geothermal Research 449 (2024) 108052

Contents lists available at ScienceDirect

Journal of Volcanology and Geothermal Research

journal homepage: www.journals.elsevier.com/journal-of-volcanology-and-geothermal-research

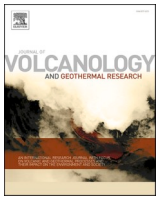

Spatiotemporal deformation and activity distribution of Irazú and Turrialba volcanoes, Costa Rica: Are these volcanoes interconnected?

Cyril Muller [a,*], Guillermo E. Alvarado [b], Mario Angarita [c], Geoffroy Avard [a]

[a] Observatorio Vulcanológico y Sismológico de Costa Rica (OVSICORI-UNA), Universidad Nacional, Costa Rica
[b] Geociencias, Instituto Costarricense de Electricidad, Apdo. 10032-1000, Costa Rica
[c] Geophysical Institute and Department of Geosciences, University of Alaska Fairbanks, Fairbanks, AK, USA

ARTICLE INFO

Keywords:
Geodetic monitoring
Eruption
Irazú
Turrialba volcano
Magma reservoir
Leveling

ABSTRACT

The spatiotemporal distribution of volcanic activity poses a significant challenge to risk mitigation measures, as it is still largely unexplored in most of the volcanic systems. In this study, we re-assess the deformation observed by leveling surveys covering the nationwide tragedy 1963–1965 Irazú eruption in Costa Rica with a state-of-the-art analytical source inversion model. We combine the analytical model results with recent geophysical, geochemical, and petrology data to build a geological model of Irazú and its 10 km-distant Turrialba volcano. Based on the leveling survey, the source inversion model finds a reservoir between 5 and 7 km below the Irazú crater which is deeper than previously published. We also confirm that the source location is on top of the mid-crustal reservoir that was feeding Turrialba between the 2010–2022 eruptions. Using previous seismic tomography, gravity, petrology, and geochemistry study of Turrialba and Irazú, as well as other studies conducted on nearby volcanoes worldwide, we find that Irazú and Turrialba volcanoes likely share a mid-crustal plumbing system which could suggesting that their plumbing systems are interconnected with each other. These findings have important implications on the spatiotemporal distribution of the volcanic activity and for the 2.8 million inhabitants settled within a 50 km radius. Observations during recent episodes indicates that inflation beneath Irazú has the potential to trigger eruptive activity at either Irazú or Turrialba. While further analysis is required to assess the tectonic control on volcanic activity, tectonic processes may shape both short- and long-term volcanic activity. These results have global implications for risk mitigation measures for nearby volcanoes.

1. Introduction

An understanding of the spatiotemporal distribution of volcanic activity and what controls it is of the utmost importance to anticipate the eruption's location, size, and timing. Yet, it mainly remains unknown or with important oversight on most of the volcanic systems. Its relevance was recently illustrated by the 2021 La Palmas eruption on Canary Island (Carracedo et al., 2022) and the 2022 Mauna Loa eruption (USGS report). In the first case, a 20 km-long rift zone fed 8 eruptions during the last 6 centuries with no apparent spatiotemporal correlation. The 2021 eruption emitted lava 16 km further north than the previous eruption. A few months before the 2021 eruption, the location of the erupting site remained uncertain (Fernández et al., 2022). Geophysical observations detected a minimum of 2 very shallow dikes up to 8 km from the 2021 vent. In the second case, Mauna Loa and the 30 km distant Kilauea volcano have shown close interaction and even an anticorrelated eruptive behavior pattern (e.g., Jaggar, 1912; Klein, 1982). Klein (1982) showed that an eruptive activity on Kilauea prolonged Mauna Loa repose time. In the last decade, Mauna Loa was inflating but had not erupted since 1984, while the Kilauea volcano was almost continuously erupting. Whether Mauna Loa and Kilauea share the same deep reservoir is still debated, but recently Gonnermann et al. (2012) showed that stress changes within a thin, porous layer (i.e., magmatic reservoir) could explain the anti-correlation between volcanoes. Przeor et al. (2022) differed on the controlling mechanism and suggested that stress changes due to the inflation of a reservoir in one volcano might control the volcanic activity on the other, without the need for a connected plumbing system. This phenomenon mirrors findings at Eyjafjallajökull in Iceland, as detailed by Albino and Sigmundsson (2014), highlighting similar volcanic dynamics. Setting aside the controversy raised by Przeor et al. (2022), inferring the location, geometry, and process controlling the plumbing system could provide an understanding of the

* Corresponding author at: OVSICORI-UNA, Campus Omar Dengo, Heredia, Costa Rica.
E-mail address: cyril.muller@una.cr (C. Muller).

https://doi.org/10.1016/j.jvolgeores.2024.108052
Received 20 July 2023; Received in revised form 14 March 2024; Accepted 17 March 2024
Available online 19 March 2024

spatiotemporal distribution of volcanic activity on nearby or extended volcanic systems.

Irazú and Turrialba volcanoes in Costa Rica are referred to as two distinct volcanoes, yet they share a common basement, and their craters are only 10 km distant. This promiscuity created legitimate fear and questions from the population of Costa Rica about the possibility of reactivation of Irazú when Turrialba started a new eruptive period in 2010–2022, particularly among the 2.8 million inhabitants (~60% of the population of the country) within 50 km around both volcanoes. Irazú forms a complex andesitic shield with about a dozen N-S aligned cusp and adventitious craters and pyroclastic cones as well as several avalanche calderas. Turrialba has only three well-defined cuspidal craters, NE-SW aligned, but several remnants and two adventitious pyroclastic cones as well as two avalanche calderas (Alvarado et al., 2006). Irazú has a larger volume and is twice as old as Turrialba (Table 1). Stratigraphic studies include tephra deposits, lava flows, lahars, and debris avalanche deposits indicating frequent activity on both volcanoes during the last 50 ka, although of different frequencies and styles. During the upper Holocene, Irazú eruptions are more frequent than Turrialba's, with an average recurrence period of 110 years and 230 years, respectively. In terms of eruption style, Turrialba produced up to Plinian and sub-Plinian eruptions, while Irazú eruptions are less explosive (Alvarado et al., 2020, Alvarado, 2021). Irazú is on a trans-extensive tectonic regime while Turrialba is on a trans-pressive regime (Calvo et al., 2019 Alvarado et al., 2021) (Fig. 1). Petrological data of the 1963–1965 eruption shows that Irazú magma ascended in months to years (Ruprecht and Plank, 2013), while Turrialba 1864–1866 and 2010–2022 eruptions showed a decade long re-awakening (i.e., 16 and 24 years, respectively) (Martini et al., 2010; Alvarado et al., 2021). The basaltic to andesitic magma component is similar for both volcanoes in the Upper Holocene, but slightly more acidic at Turrialba (Reagan et al., 2006), although some Irazú banded tephras are more silicic (Alvarado et al., 2006). During the 1963–1965 Irazú eruption, leveling data inverted using a point source model (Mogi, 1958) suggests a pressure source located about 1–2 km b.s.l. beneath the Irazú summit (Murata et al., 1966).

Table 1
Comparison of the major characteristics of Irazú and Turrialba volcanoes.

Characteristics	Irazú	Turrialba
Elevation (m a.s.l.)	3427	3325
Height above lowland (m)	3200	2900
Area (km^2)	700	663
Volume (km^3)	359	300
Estimated age of the most recent volcanic edifice (ka)	200	100
Historical eruptions	1723–1724, 1917–1921, 1924, 1928–1930, 1933, 1939–1940, 1963–1965	1864–1866, 2010–2022
Recurrence period of eruptions in years (a) for the last 2.6 ka	36–120 (average: 110)	62.5–319 (average: 230)
Re-awakening time before eruption (years)	<4	16–24
Eruptive style	Strombolian to vulcanian	Strombolian to Plinian
SiO_2 wt% in Upper Holocene (*banded tephra)*	51–58 *(58.6–63)*	50.5–61.7
Basalt composition	Unusual high-Nb concentrations (OIB)	
Petrological composition	Similar Sr and Nd isotopic compositions	
Tectonic regime	Trans-extensive	Trans-pressive
Shallow magma storage	Sea level below its crater	Various depths below the crater
Mid-crustal magma storage	9–15 km b.s.l.	6–17 km b.s.l.
Seismological and Geodetic observations	Low seismic velocity and gravity zone, 5 to 10 km below the summit, between Irazú and Turrialba	Inflation pattern detected at Irazú during the 2010–2022 Turrialba eruption; migration of seismicity from Irazú toward Turrialba during the latter's eruption.

Petrological and geophysical observations provide indications in favor of a possible interaction between the two volcanoes' plumbing systems. Both volcanoes have basalts with high Nb concentrations like those of intraplate basalts, similar Sr and Nd isotopic compositions, as well as, major, minor, and trace elements of rocks and glass compositions (Feigenson and Carr, 1986; Reagan and Gill, 1989; Alvarado, 1993; DeVitre et al., 2019). The seismological and geodetic data provide more substantive evidence of a potential connection between these volcanoes. Both volcanoes share a region of low seismic velocity and gravity zone in the upper crust (5 to 10 km below the summit), which is interpreted as a magma storage region (Husen et al., 2003; Lücke et al., 2010; Jiwani-Brown et al., 2022). The migration of volcano-tectonic seismicity from the western flank of Irazú toward Turrialba during Turrialba's eruption (2015–2016) suggests a magma injection from the mid-crust below Irazú to a shallow level below Turrialba (van der Laat et al., 2022). Between 2014 and 2016, a continuous GPS network spread over Turrialba and Irazú detected an inflation pattern centered on Irazú while Turrialba was erupting (Battaglia et al., 2019).

Although, the migration of volcano-tectonic seismicity from Irazú to Turrialba, the shared low velocity zone between Irazú and Turrialba, as well as the inflation pattern at Irazú during Turrialba's eruptive phase point toward an intricated magmatic system, it is not clear whether the Irazú and Turrialba volcanoes are two nearby but separated volcanoes or if they interact or share part of their plumbing system. However, amidst the 1963–1965 Irazú eruptive period, deformation was detected between the 1958 leveling survey and two leveling surveys in 1964 (Murata et al., 1966). Through the application of state-of-the-art models, the 1958–1964 leveling data has the potential to unravel new insights into the dynamic interplay between the volcanoes. Until recently, the crucial leveling observations were buried in some archives and only Murata et al. (1966) indications on the source were available. However, after some investigations, we have finally uncovered the original results. In this study, we feed analytical models with the disclosed 1963 leveling surveys to infer the parameters of the source generating this deformation. Then, a rigorous comparison is conducted between the resulting source parameters and those obtained in 1966. Additionally, we compiled in the same reference frame, the modeled source with the deep magma reservoirs inferred from the 2014–2016 deformation signal which accompanied the 2010–2022 Turrialba eruption as well as the most important previous geochemical, petrological, and seismic studies. This comprehensive analysis provides critical insights to outline a topological model of the Irazú and Turrialba plumbing system. We discuss the possibility of a shared-deep plumbing system between the two contiguous volcanoes and the process controlling the spatiotemporal activity on the Irazú and Turrialba volcanic system (ITVS) and its implications for risk mitigation measures.

2. 1963–1965 Irazú eruption and 1958–1964 leveling data

Irazú volcano exhibited signs of reactivation in 1959 when three active fumaroles burst from the crater walls and floor (Barquero, 1976). This was followed by the observation of a steam column on August 9, 1962. Subsequently, in January 1963, after 23 years of inactivity, the Irazú volcano entered an eruptive phase. At 13:20 of March 13th, three great eruptions in rapid succession resulting in a mushroom-shaped cloud of ash as well as incandescent lithics initiated the eruptive phase. The eruption commenced with the emission of ash and scoriaceous lapilli, which gradually increased in frequency and intensity (Gutiérrez, 1963; Barquero, 1976). On March 17th, ash began to fall on San José, the capital of Costa Rica (Gutiérrez, 1963; Barquero, 1976). The heightened volcanic activity led to the evacuation of workers and

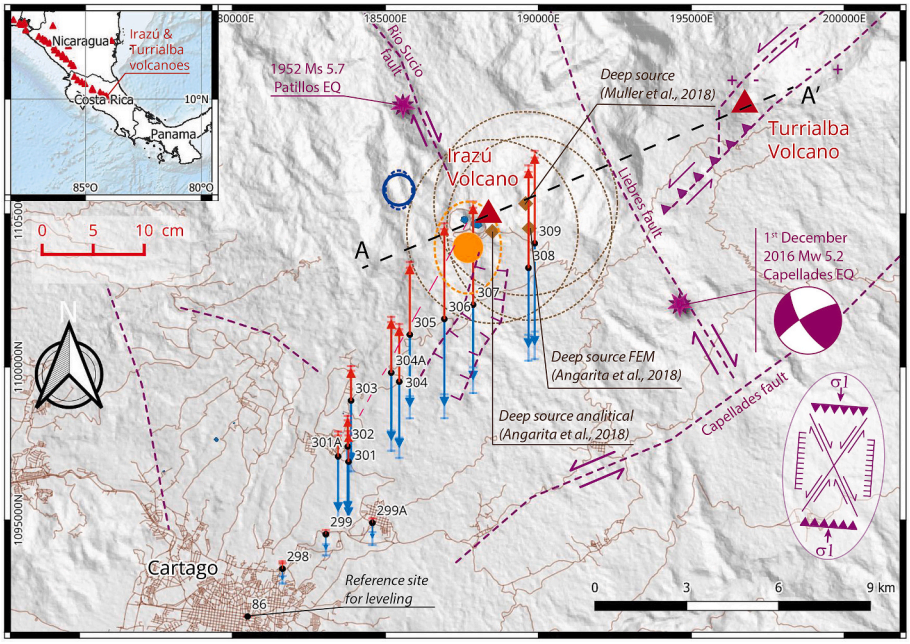

Fig. 1. 1958–1964 leveling data, modeling, and tectonic settings on Irazú and Turrialba volcanoes in Costa Rica. The small inset at the left shows a general view of the Central American isthmus and its volcanic arc (red triangles) and the location of ITVS. In the main inset, the black dots show the 15 main leveled sites observed in 1958, May 1964, and September 1964. The vertical arrows and their error bars show the deformation between 1958 and May 1964 (red) and May and September 1964 (blue) and their respective estimated standard deviation. The red scale on the left of the figure is used to size both red and blue vectors. For the sake of clarity, the figures include only the main sites. However, all the data are included in the supplementary materials A and B for a comprehensive examination. The filled orange circle shows the position of our spherical best-fit model for the period 1958- May 1964. The orange dashed ellipse shows its uncertainty based on the red arrows. The blue circle and blue dashed ellipse show the position of the best-fit model for the period May to September 1964 and its uncertainty based on the blue arrows. The brown diamond shows the position of the best-fit models for Turrialba eruption based on Angarita and Muller (2018), Muller (2018), and Battaglia et al. (2019). The purple stars show the location of the last two major earthquakes that occurred in the area and the dashed purple line shows the major faults and their kinematics when known. At the bottom right, the shear diagram of Riedel (1929) shows the main direction of the tectonic stress on the area. The black dashed line shows the cross-section of Fig. 5. The grey lines show the height contour lines every 100 m. The light brown lines show the main roads. (For interpretation of the references to colour in this figure legend, the reader is referred to the web version of this article.)

cattle on Irazú's northern flank, as ash and scoriaceous lapilli were continuously ejected (Murata et al., 1966). In April 1963, the western flank up to 15 km of the crater was covered with several centimeters of ash. From May 1963 to December 1964, steady climatic eruptions (up to 10 km above the crater) and intense ash-falls were observed with only short periods of hiatus or low activity. Lahars reaching the second city of the country, Cartago, were also frequent. The December 9th, 1963, lahar was the most destructive and deadly. Then the volcanic activity gradually diminished by the end of 1964, and ash eruptions ceased in February 1965 (Krushensky and Escalante, 1967). By July of that year, a lake had formed at the bottom of the crater, marking the end of the eruptive phase. The 1963–1965 eruptions had far-reaching consequences, impacting the local population, livestock economy, agriculture, and infrastructure (Murata et al., 1966; Alvarado et al., 2021).

During this eruptive phase, notable deformation at Irazú volcano was discovered through two leveling surveys conducted in 1964. The leveling data, though initially lost in archives, were rediscovered during this study. Our interview with Mr. Sergio Loaiza Vargas, a surveyor involved in these surveys, provided firsthand insights into the methodology. In total, 49 benchmarks were observed along the 30 km road from Cartago to Irazú ranging in altitude from 1426 to 3200 m (Supl. Mat A and B). Among these 49 leveling sites, 15 sites were previously leveled in 1958 which allows us to estimate the 1958 to May 1964 volcano deformation (Fig. 1). The null deformation was set to the furthest site (site 86). Between 1958 and May 1964, changes were inferior to 8 mm up to site 299 A (at 10.4 km to the crater). The deformation grew steadily between site 299 A and site 307 (2.3 km to the crater), then slightly decreased closer to the crater. The deformation reached up to 109 ± 14 mm on site 307 (Table S1). The 49 benchmarks were re-observed in September 1964, revealing that in most locations' subsidence was larger than the previous uplift, although this was not the case for all points. Near the volcano, three sites (306, 307, 308) exhibited subsidence that was not larger than the previous uplift, and at one additional site (305), the difference was possibly within the margin of error (Table S1). The closest benchmark to Irazú Crater showed a subsidence of −123 ± 15 mm (Table S2). Lower sites, such as 301 A and 302, showed subsidence of 35 ± 9 mm and 39 ± 10 mm below their 1958 levels, respectively. These observations suggest that the uplift observed earlier had largely dissipated within a span of four months.

Before modeling, we set the accuracy and the exact coordinates of each site. The accuracy is calculated using the Vanicek et al. (1980) equation and ranges from 3.8 mm for first class, first order leveling to 15 mm for first class but third order (Supl. Mat C). The height differences were calculated from two leveling lines and the accuracy needs to be multiplied by the square root of two to account for error propagation (Ghilani, 2017, chapter 6). Since there is no site reliably located in a non-deforming area, the farther away (site 86) from the deforming area has been set as the reference level. The small observed deformation, between 3 and 7 mm, on the first 5 km of the road from Cartago to the crater, followed by a sharp increase closer to the crater, suggests that site 86 was, indeed, in an area with little to no influence from the magmatic system. The locations of the leveling sites, while not defined in cartesian coordinates, were accurately determined based on their distances along the road, which is meticulously mapped on Irazú's southern flank. This data was then systematically transformed from the road coordinate system to a standard east-north projected system for precise geolocation (Table S1).

3. 1958–1964 leveling surveys model and results

We use dModels (Battaglia et al., 2013) to estimate the location and volume change of the magmatic sources during uplift and subsidence. dModels performs analytical inversion of geodetic observations in a homogenous elastic half-space, using a combination of a random grid search and weighted least square algorithms, with chi-squared as a penalty function. The standard deviation of the parameters is estimated through a Monte Carlo simulation (Press et al., 2007), adding Gaussian white noise to the original dataset. The noise is calculated based on the standard deviation of the observed data, and assuming a diagonal data covariance matrix. The code to model a finite sphere shape with a topographic correction (Williams and Wadge, 1998) was adapted to model only vertical displacement. Complex shapes such as ellipsoids and sills can be modeled, but a simple sphere was used to limit the number of parameters.

We modeled the deformation data with two levels of precision, specifically using 1st-order and 3rd-order leveling accuracy based on Vanicek et al. (1980) (Suppl. Mat. Table S2). Standard deviations and chi-squared (c2) values change largely using 1st-order (χ^2:9.7) or 3rd-order accuracy (χ^2:0.6), but source parameter changes are minor. Although the standard deviations on the magmatic source are larger with 3rd-order leveling accuracy, we prefer a looser stochastic model because its lower chi-squared might estimate more realistic standard deviations. During the first period, the spherical source is located less than a kilometer from the active crater, with a depth of approximately 2.4 km b.s.l. and a volume change of 16 million cubic meters (Table 2). During the second period, the deflating source on the northwestern flank is about 2.3 km from the crater, at a depth of 3.6 km b.s.l., with a volume change of −32 million cubic meters.

4. Discussion

4.1. Oversight of the magma volume

Regarding the modeled volume changes, the May to September 1964 model inferred twice the volume in deflation than the 1958-May 1964 model infers in inflation. The observed differences in model outcomes may partly stem from the model's inherent errors, compounded by the limited number of sampling points and the restricted spatial coverage of our study, which could introduce a notable sampling bias. Nevertheless, a larger source of uncertainty exists due to the lack of temporal resolution of the leveling observations. The onset of the eruption was in March 1963 while the leveling monitoring started in May 1964 (Murata et al., 1966). This raises the question: was the recorded May 1964 uplift the largest uplift experienced by the volcano? Did the volcano experience a larger deformation before May 1964 (Fig. 3)? Considering that the records of the monthly removed ash from San Jose downtown indicate the climax of the eruption between December 1963 and January 1964 (Murata et al., 1966) and that between May and September 1964 the deformation returns to almost 1958 level which implies quick feedback between magma reservoir and the superficial activity, the deformation might have been larger before May 1964. This is also supported by petrological studies that established that the magma of Irazú during its last eruption ascended at a speed between 80 and 55 m/day (Boyce and Hervig, 2009; Ruprecht and Plank, 2013; Oeser et al., 2018). Based on the depth of our modeled reservoirs (5.8–7.1 km below the crater) and these velocities, the magma may have reached the surface in 2–4 months. Together these visual, petrological, and geodetic observations suggest that the sparse time coverage of the leveling monitoring might have overlooked the deformation occurring between 1958 and May 1964. The deformation might have been more important before the May 1964 leveling and the total volume might have been significantly larger than modeled in this study. Does this conclusion also impact the position of the reservoir? Not necessarily, the plumbing system is thought to be stable over such a short period. Additionally, we explored the stability of the reservoir through an inversion model where we fixed the source geometry to the position of the reservoir during the inflation period and varied only the volume change. The results indicate a higher but acceptable fit with Chi-square value of 5 (previously $\chi^2 = 2.8$) (Fig. S1). The deflation phase volume change was estimated at −16.1 Mm^3 (previously −15.5 Mm^3), closely matching the inflation phase within the error margin. These findings imply that while the deformation intensity prior to May 1964 could have been greater than recorded, the reservoir's position likely remained stable, supporting the notion of a consistent plumbing system during this period.

Table 2
Results of the inversion model using a finite sphere shape with a topographic correction based on 1958–1964 leveling surveys.

Model	Precision	Dist. to crater [km]	Depth [km]	Volume change [Mm^3]	χ^2
1958- May 1964	1st-order	0.9 ± 0.4	2.4 ± 0.1	15.6 ± 1.2	9.7
1958- May 1964	3rd-order	0.9 ± 1.7	2.4 ± 0.7	15.5 ± 7.7	0.6
May-Sept. 1964	1 s-order	2.7 ± 0.1	3.6 ± 0.1	−34.1 ± 0.9	42.4
May-Sept. 1964	3rd-order	2.3 ± 0.7	3.6 ± 0.3	−31.5 ± 3.7	2.8

4.2. Turrialba-Irazú plumbing system

Analytical models using topography were conducted to determine the position and depth of a magma reservoir feeding the Irazú eruption. The models used a 3D analytical approach instead of the 1D point source model used by Murata et al. (1966). The models found an inflating reservoir below the crater at a depth of 2.4 km b.s.l (5.8 km below the crater) from 1958 to May 1964, and a deflating reservoir on the northwestern flank at a depth of 3.6 km b.s.l (7.1 km below the crater) from May to September 1964. The difference in depth and position of the reservoirs may reflect either the accuracy of the model or a more intricate plumbing system. However, relying solely on vertical deformation has limitations, as minor changes can lead to a range of source locations (Dieterich and Decker, 1975), so this difference likely indicates the accuracy of the models and the spatial sampling's limited resolution. The modeled depths show a 1–3 km deeper magma reservoir than previously reported by Murata et al. (1966)) but align closely with petrological and tomographic studies (Alvarado et al., 2006; Jiwani-Brown et al., 2022). The location of this magma storage is also 4–15 km above the mid-crustal reservoir, which has fueled the Turrialba eruption from 2010 to 2022, as inferred from analytical and finite element models based on continuous GNSS data (Muller, 2018; Angarita and Muller (2018); Battaglia et al., 2019) (Fig. 2). The overlapping position between the 1963–1965 Irazú feeding reservoir and the 2010–2022 Turrialba reservoir raises the question: Are the magmatic plumbing systems of Turrialba and Irazú connected?

Geochemical, geodetic, seismic, and petrological data have estimated the depth of the magma storage of each volcano below average ground altitude (3000 m). For Turrialba, De Moor et al. (2016) based on CO_2-rich gas pulses, inferred a mid-crustal reservoir at 5–7 km below sea level (b.s.l.) and a shallow reservoir between sea level and 2 km b.s.l. Di Piazza et al. (2019) interpreted a deep magma reservoir at 10 km b.s.l. from the andesitic magma involved in the ~2 ka Plinian Turrialba eruption. Conde et al. (2014) inferred very shallow magma storage (<1 km) and 1–3 km b.s.l. reservoir. For Irazú, Alvarado et al. (2006) suggest that 2 magma storages coexist, a mid-crustal reservoir at a depth between 9 and 12 km b.s.l. and a shallower reservoir at sea level. Benjamin et al. (2007), based on H_2O entrapment pressure, suggest a 3 km b.s.l. Jiwani-Brown et al. (2022) provide seismic tomography data spanning from sea level to 12 km b.s.l., revealing a low-velocity zone under Irazú

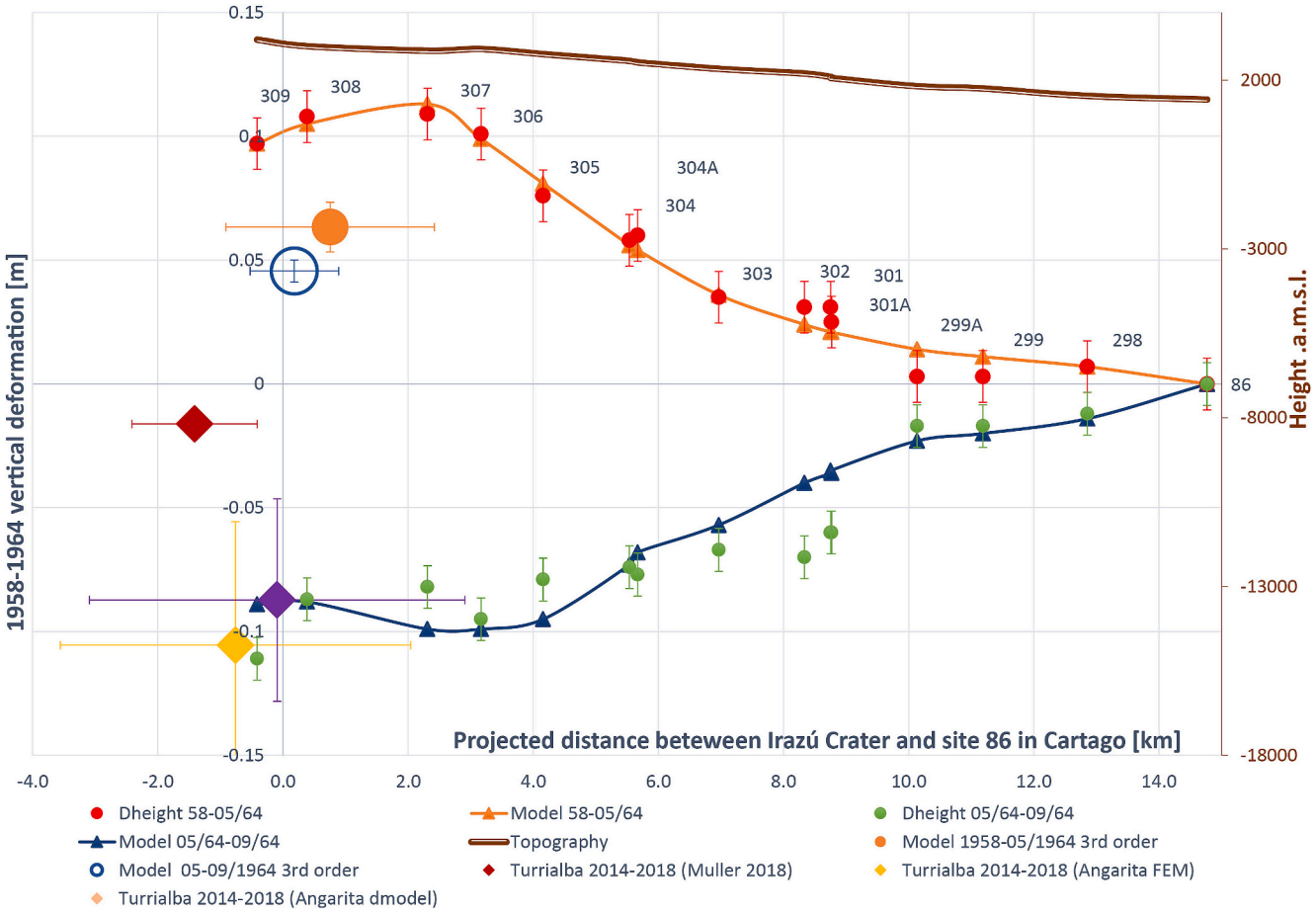

Fig. 2. Observations and models of the vertical deformation between 1958 and 1964 as well as the models based on the 2014–2016 Turrialba deformation. The graph presents two distinct data sets: the deformation, left axis, and the elevation and depth of the models and leveling sites, right axis. The horizontal axis represents the projected distance between Cartago and the Irazú crater. Referred to the left vertical axis, the red dots represent the deformations between 1958 and May 1964 and their standard deviation. The orange triangles and line depict the results of the best-fit model for the same period. In contrast, the green dots illustrate the deformation between May 1964 and September 1964 and its standard deviation. The blue triangles and lines represent the results of the best-fit model for the same period. For the sake of clarity, the figures include only the main sites. However, all the data are detailed in the supplementary materials A and B for a comprehensive examination. On the elevation and depth axis (right), the brown double lines indicate the altitudes of the sites. The large orange dot and blue circle mark the positions of the best-fit model for the 1958 and May 1964 period and the May 1964 and September 1964 period, respectively. The diamonds represent the best magmatic source model associated with the Turrialba eruption during the period 2015–2016. The red, purple and yellow diamonds show the position of the analytical model of Muller (2018), the analytical model of Angarita and Muller (2018), and the finite element model of Angarita and Muller (2018), respectively. The error bars show the estimated standard deviation for each model. (For interpretation of the references to colour in this figure legend, the reader is referred to the web version of this article.)

and Turrialba from 0 to 4 km deep. Below, the anomaly narrows, both in the SW-NE and NW-SE axis, concentrating directly beneath Irazú's crater. This zone is interpreted as potential magma storage area. This anomaly is surrounded by a clear shift to higher-velocity materials (Fig. 4). The same study does not show strong evidence of well-developed magma storage below the Turrialba summit area. The 4–8 km b.s.l. magma storage also fits with Lücke et al. (2010) low-density body. In summary, all these studies indicate shallow magma storage below volcano craters, although, Turrialba might have a series of small zones of magma storages rather than one well-developed region. Additionally, both volcanoes have deeper magmatic reservoirs, in an overlapping depth of 5–17 km b.s.l. for Turrialba and 4–12 km b.s.l. for Irazú, located below Irazú crater or between the two volcanoes.

In their study, Rouwet et al. (2021) proposed a hydrogeological connection between Turrialba and Irazú volcanoes, inferred from the observed decrease in the water level of Irazú's crater lake coinciding with Turrialba's reawakening. However, this hypothesis encounters several challenges. Firstly, Ramírez et al. (2013) documented instances where the lake underwent cycles of drying and refilling independent of any volcanic activity at Turrialba. Additionally, an alternative explanation for the lake's drainage could be attributed to the northern volcanic cave, situated <500 m away. Moreover, the presence of the Liebres fault, acting as a geological barrier, likely impedes any significant hydrological interaction between the two volcanoes.

Within a global dataset, a significant proportion of proximal volcanoes exhibit interconnected magma plumbing systems, indicative of a prevalent geological feature among closely spaced volcanic systems (Biggs et al., 2016). Volcanoes such as Alu and Dalafilla in Ethiopia (6 km apart), where pre-eruptive inflation was observed under Alu alone, but co-eruptive subsidence extended 10 km toward Dalafilla, suggesting a common plumbing system (Pagli et al., 2012). In Iceland, the Eyjafjallajökull and Fimmvörðuháls volcanoes, (8 km apart) experienced a notable eruption sequence in 2010. The eruption started at Fimmvörðuháls and a month later, Eyjafjallajökull erupted (Sigmundsson et al., 2010; Tarasewicz et al., 2012). Prior to the Fimmvörðuháls eruption, there was a migration of seismicity from Eyjafjallajökull, the main volcano, to Fimmvörðuháls. This pattern was similar to what van der Laat et al. (2022) detected between 2015 and 2016 in ITVS. Cordón Caulle and Puyehue volcanoes in Chile, located 6 km apart, not only share an extensive, long-lived crystal-rich zone at a depth of 4–7 km (Jay

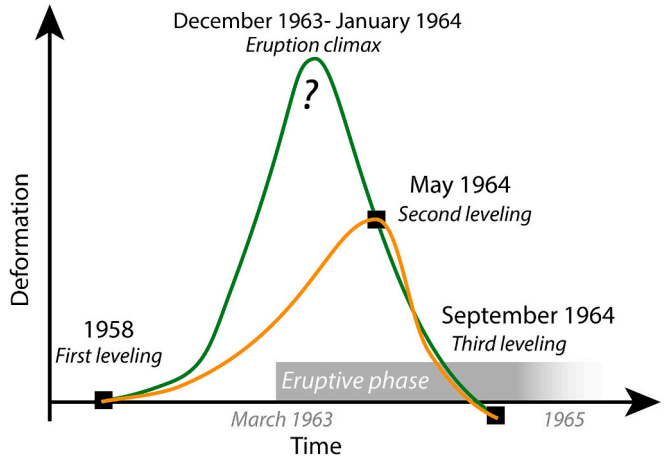

Fig. 3. Uncertainties on the volcano deformation. Compared to the 1958 leveling. Was the recorded May 1964 uplift, the largest uplift experienced by the volcano? Or did the volcano experience a larger deformation before May 1964? The green curve shows the scenario where the volcano experienced a larger deformation before 1964, the date of the second leveling. The orange curve shows what we can infer from the geodetic observation. (For interpretation of the references to colour in this figure legend, the reader is referred to the web version of this article.)

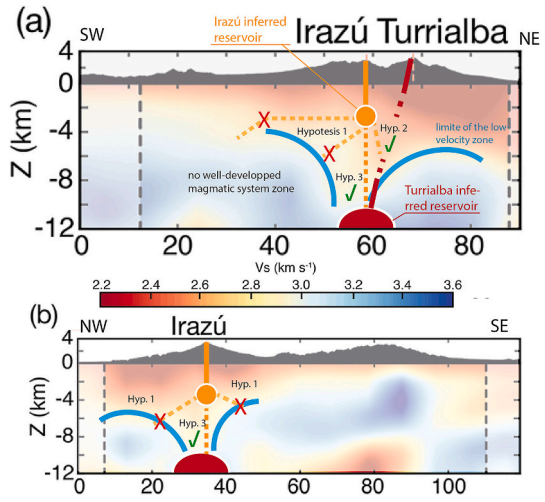

Fig. 4. Evaluation of hypotheses concerning the magma supply to Irazú's shallow crustal reservoir regarding seismic velocity changes by Jiwani-Brown et al. (2022). The colour scale illustrates the seismic velocity changes (Vs). The inferred reservoirs for Irazú and Turrialba are marked by solid orange and solid red ellipses, respectively. Blue curves outline the low-velocity zone identified by Jiwani-Brown et al. (2022). A red line schematically indicates the magma supply route to Turrialba's crater, with a dashed line highlighting the associated uncertainties. Orange lines depict the magmatic plumbing system beneath Irazú, whereas orange dashed lines explore different hypotheses regarding this system. Hypothesis 1 is considered unlikely, with Hypotheses 2 and 3 being the predominant theories for the magma supply pathway to Irazú's shallow reservoir. Subplot a) shows a SW-NE cross-section, while subplot b) shows a NW-SE cross section. This illustration is adapted from Fig. 9 in Jiwani-Brown et al. (2022). (For interpretation of the references to colour in this figure legend, the reader is referred to the web version of this article.)

et al., 2014) but also exhibit pre-eruptive deformation episodes that imply a widespread and interconnected magma plumbing system, extending the influence of deformation beyond the immediate vicinity of the 2011 eruptive vent. For volcanoes distant up to several tens of kilometers a common source is found deeper, for example, Arya and Kirishima volcanoes in Japan (30 km apart) and Mauna Loa and Kilauea in Hawaii share an asthenospheric reservoir (Brothelande et al., 2018, Gonnermann et al., 2012). In Iceland, at Grímsvötn, Bárðarbunga, and Holuhraun, (25 and 40 km apart respectively), geodetic observations have detected a lateral migration of the magma in 2014. In this case, the first two volcanoes share a common lower crust reservoir and the Holuhraun eruption was fueled by Bárðarbunga mid-crustal reservoir (Bato et al., 2018). Biggs et al. (2016) conclude that interaction between <10 km spaced volcanoes might highlight a common mid-crustal crystal mush layer while volcanoes more widely spaced might share a deeper source (i.e., in the asthenosphere) or interact due to stress changes.

Leveraging insights from previous ITVS studies and global volcanic observations, we can attempt to deduce the likelihood of Irazú and Turrialba having a shared plumbing system, though this inference is subject to inherent uncertainties. The 1963–1965 Irazú eruption was fed from a reservoir positioned above the mid-crustal reservoir that fueled the 2010–2022 Turrialba eruption. Irazú and Turrialba erupted material shows similar high Nb concentration (i.e., OIB signature), similar Sr and Nd isotopic composition, as well as share some major, minor, and trace elements in rocks and glass compositions (Alvarado, 1993; Feigenson and Carr, 1986; Reagan and Gill, 1989; DeVitre et al., 2019). Both volcanoes have a mid-crustal reservoir, in an overlapping depth of 4–17 km b.s.l (Alvarado et al., 2006; Di Piazza et al., 2019). Gravity and seismic tomography reveal unique distinctive low gravity and velocity anomalies located below Turrialba and Irazú (Lücke et al., 2010; Jiwani-Brown et al., 2022). Furthermore, from 4 to 12 km b.s.l. the detected low-velocity anomaly narrows and is centered below Irazú's crater, just on top of the inferred mid-crustal reservoir of Turrialba (Fig. 4). Given the well-developed and mature volcanic system of Irazú, we would typically anticipate identifying a distinct low-velocity anomaly as evidence of a lateral shift in the volcano's plumbing system (as postulated in Hypothesis 1 from Fig. 4). Yet, such an anomaly is absent. Therefore, Irazú feeding system might be sub-vertical or exhibit a lateral extension toward the west or north (Hypothesis 2 and 3 from Fig. 4). Regardless of the directional orientation, the funnel-shaped low-velocity zone suggests that Irazú's magmatic supply is likely to intersect with the Turrialba mid-crustal reservoir beneath Irazú crater. This interpretation is in line with global observations, where adjacent volcanoes frequently share a common reservoir. Moreover, the ratio distance between volcanoes and depth of a potential shared reservoir at ITVS corresponds with patterns noted in other volcanic systems (Biggs et al., 2016). Ultimately, global volcanic observations, alongside prior research on Turrialba and Irazú, hint at the possibility of an interconnected magmatic system. Although, this concept necessitates additional corroborative research, including petrological analyses or identifying an inflating mid-crustal reservoir before the next eruption at Irazú volcano.

This new paradigm model might have direct implications for risk management and the spatiotemporal distribution of the eruptive activity at ITVS. Although the volcanoes might share a common mid-crustal reservoir, their shallow plumbing systems evince disparity, thereby exerting an influence on the spatiotemporal distribution of volcanic activity. Irazú, that might be characterized by minimal or no horizontal displacement to a mid-crustal reservoir, exhibits a pattern of frequent yet less intense eruptions and shorter eruptive durations compared to Turrialba. However, the rapid magma ascent (e.g. (Ruprecht and Plank, 2013) implies few precursory signals before an eruption. In contrast, Turrialba with its suggested 10-km offset with the main reservoir, might not have develop an efficient magma pathway. Therefore, it has a long reawakening period with a plethora of detectable precursors (i.e., seismicity, gas, deformation, …) (e.g. Martini et al., 2010; Alvarado et al., 2021). Ineffectual magma transport may also give rise to many thwarted eruptions, consequently affording extended inter-eruptive intervals. However, small magma batches emplaced during earlier eruptions can evolve toward more silicic melt (e.g. DeVitre et al., 2019) and if the subsequent eruption is capable of drawing upon a significant volume of these very same batches, an explosive eruption may ensue, alike El Retiro Plinian eruption two millennia ago.

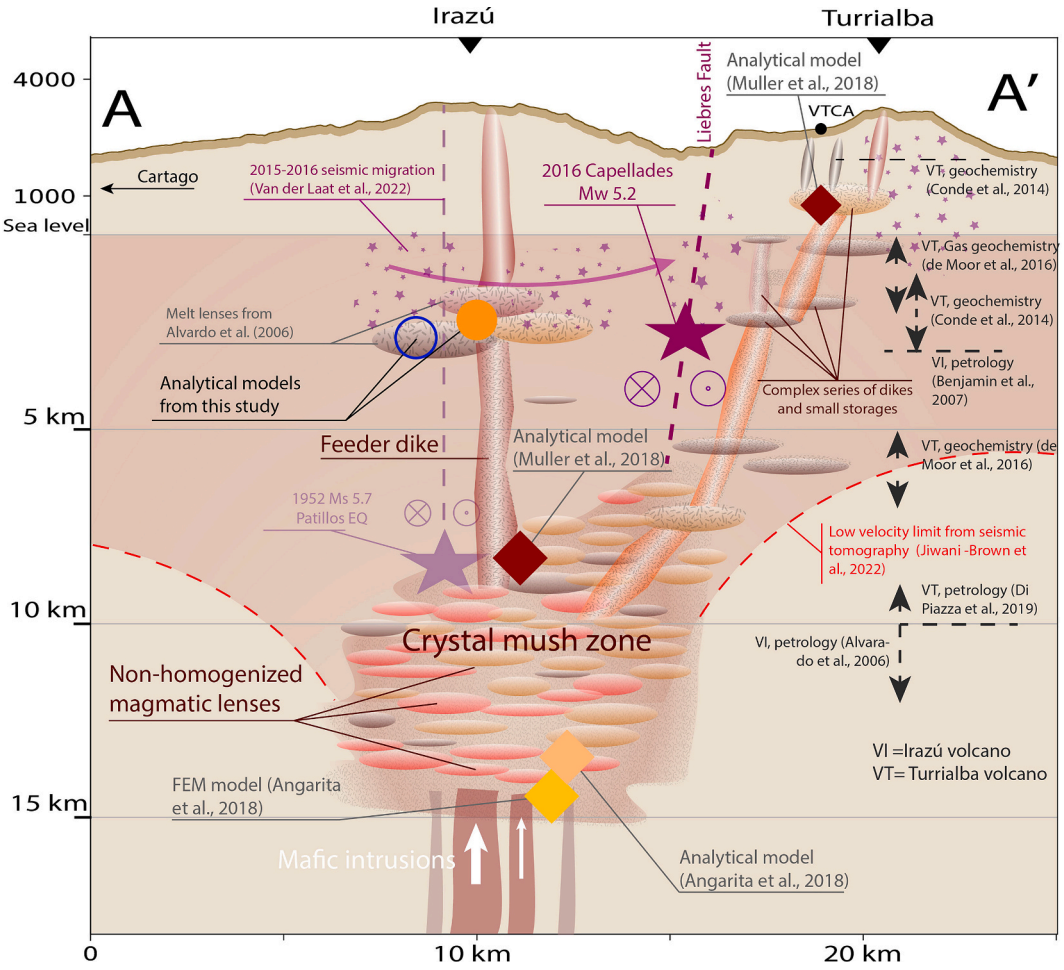

Fig. 5. Schematic topological model of ITVS plumbing system from the results of this work as well as all other studies that have published geometrical parameters of ITVS. The seismic data are in purple. The group of stars indicates the position of the 2015–2016 volcano-tectonic swarm based on van der Laat et al. (2022). The diamond indicates the position of the sources modeled by Muller (2018) and Angarita and Muller (2018) while the orange dot and blue circle are the results of the 1958–1964 leveling inversion. The position of the Capellades and Patillos earthquakes (large purple stars) are from Linkimer et al. (2018) and Montero et al. (2013). (For interpretation of the references to colour in this figure legend, the reader is referred to the web version of this article.)

4.3. Processes controlling Irazú and Turrialba eruption

A possible shared reservoir feeding both volcanoes brings an inquiry into the process that attends to the feeding of individual eruptions. In the instance that a novel magma injection reaches the mid-crustal reservoir, what are the mechanisms that come into play to dictate the eruption of either one or another volcano? Although, high-conductivity pathways exist between neighbor volcanoes (e.g. Brothelande et al., 2018; Bato et al., 2018), in the crust, repetitive injections over hundreds of thousands of years result in magma reservoirs including stacked sills of magma with large diversity of chemical signature within crystalline mush zone (Cashman and Giordano, 2014). Petrological observations demonstrate that melt-rich lenses only coalesced shortly before or during an eruption, even on large eruption, which precludes the conceptual frame of one giant pre-eruptive magma chamber and simple pressure changes within a high-conductivity pathways (Wotzlaw et al., 2013; Ellis et al., 2014). This conceptual frame affords a manifold of behavior. For example, on Mauna Loa and Kilauea volcanoes, activity is anti-correlated. There is clear evidence that an increase in activity in one of the volcanoes prolongs the repose time at the other (Klein, 1982). Such behavior is observed when volcanoes are coupled through a porous reservoir where dynamic stress transfer inhibits eruptions of the adjacent volcano (Gonnermann et al., 2012). In ITVS, magma reservoirs that have evolved for hundreds of thousands of years are likely to be an intricated pile of melt-rich lenses. A new magma injection from the lower crust has the potential to perturb numerous lenses, a phenomenon that elicits a heterogeneous range of erupted products, as evinced by Alvarado et al. (2006) and DeVitre et al. (2019). The impending eruption of Irazú may unlock a valuable and more profound understanding of the underlying mechanisms that govern the preferential eruption of either volcano.

The tectonic activity might be an essential process in shaping the volcanic activity of the ITVS. Tectonic causes static or dynamic stress changes (e.g., Linde and Sacks, 1998; Diez et al., 2005; Allan et al., 2012; Pritchard et al., 2013; Bégué et al., 2014; De Moor et al., 2017). These changes can either un- or clamp dikes, increasing, releasing stress on magma reservoirs, or changing the permeability of the hydrothermal system. When an earthquake occurs an increase or decrease of the volcanic activity could be triggered (Seropian et al., 2021; Ebmeier et al., 2016). ITVS lies within a dextral pull-apart basin (Montero et al., 2013) and Irazú exhibits an N-S alignment of eruptive centers within an extensive or trans-extensive tectonic regime. On the contrary, Turrialba stands within an overall transpressive context and exhibits a NE-SW alignment of its eruptive centers (Calvo et al., 2019). In Fig. 1, all tectonic features related to these descriptions, including both basin and eruptive center alignments, are indicated by the purple features. The prevailing tectonic stress regime in the region likely played a pivotal role in modulating the subsurface magmatic configuration, promoting the accumulation of a significant magma body beneath Irazú. This same tectonic environment may have concurrently obstructed the formation

of a direct conduit and a well-developed shallow magma reservoir under Turrialba. Such tectonic influences might be critical in dictating the pathways of magma ascent, the location and ultimately, the eruptive characteristics of these volcanoes. This nuanced understanding highlights the integral role of regional tectonics in shaping the volcanic architecture and underscores the necessity of incorporating tectonic frameworks in volcanic hazard assessments and interpretations of magmatic activity. If in the long run, the predominant tectonic stress regime holds the capacity to govern the spatiotemporal occurrence of the ITVS, in the short term, tectonic activity might also rule ITVS. For example, on December 1st, 2016, a right-lateral 5.5 magnitude earthquake struck within the heart of ITVS (Linkimer et al., 2018) (Figs. 1 and 5). The two-year-long seismicity observed by van der Laat et al. (2022) (Fig. 5), ended and the rapid inflation observed between 2014 and 2016 decreased significantly as well as the ash emitted (Fig. S2, S3). While further investigations are warranted to fully comprehend the repercussions of this earthquake on ITVS activity changes, it is worth noting that tectonic activity may also exert an impact on volcanic activity in the short term, as observed in the context of other volcanoes (e.g. Ebmeier et al., 2016; Maccaferri et al., 2016; Xu et al., 2016). Upon consideration of both long- and short-term tectonic records, it is plausible that tectonic activity plays a major role in governing the spatiotemporal distribution activity of the ITVS.

5. Conclusion

In this study, we re-analyze the leveling data from 1958 to 1963 at Irazú volcanoes in Costa Rica to feed the state-of-the-art analytical model as well as the previous petrological, seismological, geochemical, and geodetic studies on both Turrialba and Irazú to uncover the characteristics of the plumbing system of both volcanoes. The newly re-analyzed leveling data shows that the deformation likely originated from a magmatic source 5–7 km below the Irazú crater. The overlapping position of this source with the mid-crustal source, which fed the 2010–2022 Turrialba eruption, as well as seismic and petrological studies, suggest that Turrialba and Irazú might be connected at depth. This possible deep-seated link provides a better understanding of the geometry of the ITVS magmatic system and clarifies the eruptive pattern of both volcanoes. Additionally, the tectonic regime gives an insight into the tectonic control on the plumbing system to contribute to our comprehension of the spatiotemporal distribution of volcanic activity and better mitigation of volcanic risks.

During a potential future eruption at Irazú novel insights into the underlying processes that facilitate the preferential eruption of one volcano over the other may be gleaned. Additionally, to further support the notion of shared mid-crustal storage, more refined petrological studies are required. For example, the comparison of the rocks, glasses, and minerals (geochemistry, isotopes, and fluid inclusions) between both volcanoes, particularly for the last two major historical eruptions of both Irazú (1723–1724 and 1963–1965) and Turrialba (1864–1866 and 2010–2021). Similarly, to the anticorrelated eruptive pattern observed between Mauna Loa and Kilauea, it would be noteworthy to assess whether the eruption of one volcano extended the dormant phase of the other. Finally, the findings of this study have major implications for the safety of the 2.8 million inhabitants settled within a 50 km radius of ITVS and as well as other volcanic systems worldwide.

CRediT authorship contribution statement

Cyril Muller: Visualization, Validation, Methodology, Investigation, Formal analysis, Data curation, Conceptualization, Writing – review & editing, Writing – original draft. **Guillermo E. Alvarado:** Visualization, Validation, Methodology, Investigation, Funding acquisition, Data curation, Conceptualization, Writing – review & editing, Writing – original draft. **Mario Angarita:** Validation, Methodology, Formal analysis, Data curation, Writing – review & editing, Writing – original draft. **Geoffroy Avard:** Visualization, Methodology, Formal analysis, Writing – review & editing, Writing – original draft.

Declaration of competing interest

The authors declare that they have no known competing financial interests or personal relationships that could have appeared to influence the work reported in this paper.

Data availability

The 1958 and 1963 leveled altitudes used in this study are available in the supplementary material. The original leveling data are in the leveling_1964_all.pdf file.

Acknowledgments

This work was supported by Universidad Nacional de Costa Rica through the project 0097-2020 “Sistema de monitoreo geodésico (SiMoGeod) de los volcanes y de la tectónica de Costa Rica.”. We thank Sergio Loaiza for his interesting and narrative experience during the last eruptive period of Irazú and their topographic survey at that time. We thank Maurizio Battaglia from USGS for adapting the dModel script to allow inverted leveling data only. We extend our gratitude to the anonymous reviewers for their time and insightful comments.

Appendix A. Supplementary data

Supplementary data to this article can be found online at https://doi.org/10.1016/j.jvolgeores.2024.108052.

References

Albino, F., Sigmundsson, F., 2014. Stress transfer between magma bodies: influence of intrusions prior to 2010 eruptions at Eyjafjallajökull volcano, Iceland. J. Geophys. Res. Solid Earth 119 (4), 2964–2975. https://doi.org/10.1002/2013JB010510.

Allan, A.S., Wilson, C.J., Millet, M.A., Wysoczanski, R.J., 2012. The invisible hand: Tectonic triggering and modulation of a rhyolitic supereruption. Geology 40 (6), 563–566. https://doi.org/10.1130/G32969.1.

Alvarado, G.E., 1993. Volcanology and Petrology of Irazú Volcano, Costa Rica. Univ Kiel, p. 261. Ph.D. thesis.

Alvarado, G.E., 2021. Costa Rica y sus volcanes. EUCR, EUNA, ETCR. ISBN: 978-9968-46-776-6.

Alvarado, G.E., Campos-Durán, D., Brenes-André, J., Alpízar, Y., Núnez, S., Esquivel, L., Sibaja, J., Fallas, B., 2021. Peligros volcánicos del Irazú, Costa Rica. Internal report of Comisión Nacional de Prevención de Riesgos y Atención de Emergencias, Costa Rica.

Alvarado, G.E., Carr, M.J., Turrin, B.D., Swiher, C., Schmincke, H.-U., Hudnut, K.W., 2006. Recent volcanic history of Irazú volcano, Costa Rica: Alternation and mixing of two magma batches, and pervasive mixing. In: Rose, W.I., Bluth, G.J.S., Carr, M.J., Ewert, J.W., Patino, L.C., Vallance, J.W. (Eds.), Volcanic Hazards in Central America (Geol. Soc. Amer., Sp. Paper), vol. 412. Geol. Soc. Amer. Inc., Boulder, pp. 259–276. https://doi.org/10.1130/2006.2412(14).

Alvarado, G.E., Esquivel, L., Sánchez, B.E., Matamoros, G., 2020. Peligro volcánico del Turrialba, Costa Rica. In: Internal report of Comisión Nacional de Prevención de Riesgos y Atención de Emergencias, Costa Rica, San José.

Angarita, M., Muller, C., 2018. Fuentes de deformación en los volcanes Irazú y Turrialba durante el periodo 2015-2016 usando datos de estaciones GPS. In: Memoria IV Congreso Nacional de Gestión del Riesgo y Adaptación al Cambio Climático, 10-11 de octubre, pp. 99–100. ISBN 978-9930-9684-0-6.

Barquero, J., 1976. El volcán Irazú y su actividad (Tesis Lic.). Esc. Ciencias Geográficas. Univ. Nacional.

Bato, M.G., Pinel, V., Yan, Y., et al., 2018. Possible deep connection between volcanic systems evidenced by sequential assimilation of geodetic data. Sci. Rep. 8, 11702 (2018). https://doi.org/10.1038/s41598-018-29811-x.

Battaglia, M., Alpala, J., Alpala, R., Angarita, M., Arcos, D., Eulliades, L., Euillades, P., Muller, C., Narvaez, L., 2019. Monitoring volcanic deformation. In: Reference Module in Earth Systems and Environmental Sciences. Elsevier B. https://doi.org/10.1016/B978-0-12-409548-9.10902-9.

Battaglia, M., Cervelli, P.F., Murray, J.R., 2013. dMODELS: a MATLAB software package for modeling crustal deformation near active faults and volcanic centers. J. Volcanol. Geotherm. Res. 254, 1–4. https://doi.org/10.1016/j.jvolgeores.2012.12.018.

Bégué, F., Deering, C.D., Gravley, D.M., Kennedy, B.M., Chambefort, I., Gualda, G.A., Bachmann, O., 2014. Extraction, storage, and eruption of multiple isolated magma batches in the paired Mamaku and Ohakuri eruption, Taupo Volcanic Zone, New Zealand. J. Petrol. 55 (8), 1653–1684. https://doi.org/10.1093/petrology/egu038.

Benjamin, E.R., Plank, T., Wade, J.A., Kelley, K.A., Hauri, E.H., Alvarado, G.E., 2007. High water contents in basaltic magmas from Irazú Volcano, Costa Rica. J. Volcanol. Geotherm. Res. 168 (1–4), 68–92. https://doi.org/10.1016/j.jvolgeores.2007.08.008.

Biggs, J., Robertson, E., Cashman, K., 2016. The lateral extent of volcanic interactions during unrest and eruption. Nat. Geosci. 9 (4), 308–311. https://doi.org/10.1038/ngeo2658.

Boyce, J.W., Hervig, R.L., 2009. Apatite as a monitor of late-stage magmatic processes at Volcán Irazú, Costa Rica. Contrib. Mineral. Petrol. 157, 135–145. https://doi.org/10.1007/s00410-008-0325-x.

Brothelande, E., Amelung, F., Yunjun, Z., Wdowinski, S., 2018. Geodetic evidence for interconnectivity between Aira and Kirishima magmatic systems, Japan. Sci. Rep. 8, 9811. https://doi.org/10.1038/s41598-018-28026-4.

Calvo, C., Madrigal, K., Merayo, F., Salazar, M., Fallas, C., Alvarado, G.E., Sánchez, B., Sánchez, R., 2019. Modelo volcanotectónico del graben cuspidal complejo del Turrialba (Costa Rica) y su relación con los colapsos sectoriales bajo un régimen transpresivo y transtensivo. Rev. Geol. Am. Cent. 61, 57–77. https://doi.org/10.15517/rgac.v2019i61.000.

Carracedo, J.C., Troll, V.R., Day, J.M.D., Geiger, H., Aulinas, M., Soler, V., Deegan, F.M., Perez-Torrado, F.J., Gisbert, G., Gazel, E., Rodriguez-Gonzalez, A., Albert, H., 2022. The 2021 eruption of the Cumbre Vieja volcanic ridge on La Palma, Canary Islands. Geol. Today 38, 94–107. https://doi.org/10.1111/gto.12388.

Cashman, K.V., Giordano, G., 2014. Calderas and magma reservoirs. J. Volcanol. Geotherm. Res. 288, 28–45. https://doi.org/10.1016/j.jvolgeores.2014.09.007.

Conde, V., Bredemeyer, S., Duarte, E., Pacheco, J.F., Miranda, S., Galle, B., Hansteen, T. H., 2014. SO_2 degassing from Turrialba Volcano linked to seismic signatures during the period 2008–2012. Int. J. Earth Sci. (Geol. Rundsch.) 103, 1983–1998. https://doi.org/10.1007/s00531-013-0958-5.

De Moor, J.M., Aiuppa, A., Avard, G., Wehrmann, H., Dunbar, N., Muller, C., Tamburello, G., Giudice, G., Liuzzo, M., Moretti, R., Conde, V., Galle, B., 2016. Turmoil at Turrialba Volcano (Costa Rica): Degassing and eruptive processes inferred from high-frequency gas monitoring. J. Geophys. Res. Solid Earth 121, 5761–5775. https://doi.org/10.1002/2016JB013150.

De Moor, J.M., Kern, C., Avard, G., Muller, C., Aiuppa, A., Saballos, A., Ibarra, M., LaFemina, P., Protti, M., Fischer, T.P., 2017. A new sulfur and carbon degassing inventory for the Southern central American Volcanic Arc: the importance of accurate time-series data sets and possible tectonic processes responsible for temporal variations in arc-scale volatile emissions. Geochem. Geophys. Geosyst. 18 (12), 4437–4468. https://doi.org/10.1002/2017GC007141.

DeVitre, C.L., Gazel, E., Allison, C.M., Soto, G., Madrigal, P., Alvarado, G.E., Lücke, O.H., 2019. Multi-stage chaotic magma mixing at Turrialba volcano. J. Volcanol. Geotherm. Res. 381, 330–346. https://doi.org/10.1016/j.jvolgeores.2019.06.011.

Di Piazza, A., Vona, A., Mollo, S., De Astis, G., Soto, G.J., Romano, C., 2019. Unsteady magma discharge during the "El Retiro" subplinian eruption (Turrialba volcano, Costa Rica): Insights from textural and petrological analyses. J. Volcanol. Geotherm. Res. 371, 101–115. https://doi.org/10.1016/j.jvolgeores.2019.01.004.

Dieterich, J.H., Decker, R.W., 1975. Finite element modeling of surface deformation associated with volcanism. J. Geophys. Res. 80 (29), 4094–4102. https://doi.org/10.1029/JB080i029p04094.

Diez, M., La Femina, P.C., Connor, C.B., Strauch, W., Tenorio, V., 2005. Evidence for static stress changes triggering the 1999 eruption of Cerro Negro Volcano, Nicaragua and regional aftershock sequences. Geophys. Res. Lett. 32 (4) https://doi.org/10.1029/2004GL021788.

Ebmeier, S.K., Elliott, J.R., Nocquet, J.M., Biggs, J., Mothes, P., Jarrín, P., Yépez, M., Aguaiza, S., Lundgren, P., Samsonov, S.V., 2016. Shallow earthquake inhibits unrest near Chiles–Cerro Negro volcanoes, Ecuador–Colombian border. Earth Planet. Sci. Lett. 450, 283–291. https://doi.org/10.1016/j.epsl.2016.06.046.

Ellis, B.S., Bachmann, O., Wolff, J.A., 2014. Cumulate fragments in silicic ignimbrites: the case of the Snake River Plain. Geology 42 (5), 431–434. https://doi.org/10.1130/G35399.1.

Feigenson, M.D., Carr, M.J., 1986. Positively correlated Nd and Sr isotope ratios of lavas from the central American volcanic front. Geology 14 (1), 79–82, 10.1130/0091-7613(1986)14<79:PCNASI>2.0.CO;2.

Fernández, J., Escayo, J., Camacho, A.G., Palano, M., Prieto, J.F., Hu, Z., Samsonov, S.V., Tiampo, K.F., Ancochea, E., 2022. Shallow magmatic intrusion evolution below La Palma before and during the 2021 eruption. Sci. Rep. 12, 20257. https://doi.org/10.1038/s41598-022-23998-w.

Ghilani, C.D., 2017. Adjustment Computations: Spatial Data Analysis. John Wiley & Sons. ISBN: 978-0-471-69728-2.

Gonnermann, H., Foster, J., Poland, M., Wolfe, C.J., Brooks, B.A., Miklius, A., 2012. Coupling at Mauna Loa and Kīlauea by stress transfer in an asthenospheric melt layer. Nat. Geosci. 5, 826–829. https://doi.org/10.1038/ngeo1612.

Gutiérrez, F., 1963. Actividad del volcán Irazú. Inf. Semestral enero-junio: 33-38. IGN, San José.

Husen, S., Quintero, R., Kissling, E., Hacker, B., 2003. Subduction-zone structure and magmatic processes beneath Costa Rica constrained by local earthquake tomography and petrological modelling. Geophys. J. Int. 155 (1), 11–32. https://doi.org/10.1046/j.1365-246X.2003.01984.x.

Jaggar, T.A., 1912. Report of the Hawaiian Volcano Observatory of the Massachusetts Institute of Technology and the Hawaiian Volcano Research Association. Society of Arts of the Massachusetts Institute of Technology.

Jay, J., Costa, F., Pritchard, M., Lara, L., Singer, B., Herrin, J., 2014. Locating magma reservoirs using InSAR and petrology before and during the 2011–2012 Cordón Caulle silicic eruption. Earth Planet. Sci. Lett. 395, 254–266. https://doi.org/10.1016/j.epsl.2014.03.046.

Jiwani-Brown, E.A., Planès, T., Pacheco, J.F., Mora, M.M., Lupi, M., 2022. Magmatic and Tectonic Domains of Central Costa Rica and the Irazú-Turrialba Volcanic complex Revealed by Ambient Noise Tomography. J. Geophys. Res. Solid Earth 127 (11). https://doi.org/10.1029/2022JB024575.

Klein, F.W., 1982. Patterns of historical eruptions at Hawaiian volcanoes. J. Volcanol. Geotherm. Res. 12 (1–2), 1–35. https://doi.org/10.1016/0377-0273(82)90002-6.

Krushensky, R.D., Escalante, G., 1967. Activity of Irazú and Poás volcanoes, Costa Rica, November 1964–July 1965. Bull. Volcanol. 31 (1), 75–84. https://doi.org/10.1007/BF02597006.

van der Laat, L., Mora, M.M., Pacheco, J.F., Lesage, P., Meneses, E., 2022. Seismicity during the recent activity (2009–2020) of Turrialba volcano, Costa Rica. J. Volcanol. Geotherm. Res. 431, 107651 https://doi.org/10.1016/j.jvolgeores.2022.107651.

Linde, A., Sacks, I., 1998. Triggering of volcanic eruptions. Nature 395, 888–890. https://doi.org/10.1038/27650.

Linkimer, L., Arroyo, I.G., Soto, G.J., Porras, J.L., Araya, M.C., Mora, M.M., Taylor, M., 2018. El sismo de Capellades del 2016 y su secuencia sísmica: Manifestación de fallamiento de rumbo en el arco volcánico de Costa Rica. Boletín Geol. 40 (2), 35–53. https://doi.org/10.18273/revbol.v40n2-2018002.

Lücke, O.H., Götze, H.-J., Alvarado, G.E., 2010. A Constrained 3D Density Model of the Upper Crust from Gravity Data Interpretation for Central Costa Rica. Int. J. Geophys. 2010 https://doi.org/10.1155/2010/860902.

Maccaferri, F., Rivalta, E., Passarelli, L., Aoki, Y., 2016. On the mechanisms governing dike arrest: Insight from the 2000 Miyakejima dike injection. Earth Planet. Sci. Lett. 434, 64–74. https://doi.org/10.1016/j.epsl.2015.11.024.

Martini, F., Tassi, F., Vaselli, O., Del Potro, R., Martinez, M., van der Laat, R., Fernandez, E., 2010. Geophysical, geochemical and geodetical signals of reawakening at Turrialba volcano (Costa Rica) after almost 150 years of quiescence. J. Volcanol. Geotherm. Res. 198 (3–4), 416–432. https://doi.org/10.1016/j.jvolgeores.2010.09.021.

Mogi, K., 1958. Relations between the eruptions of various volcanoes and the deformations of the ground surface around them. Bull. Earthq. Res. Inst., Univ. Tokyo 36, 99–134.

Montero, P.W., Lewis, J.C., Marshall, J.S., Kruse, S., Wetmore, P., 2013. Neotectonic faulting and forearc sliver motion along the Atirro–Río Sucio fault system, Costa Rica, Central America. GSA Bull. 125 (5–6), 857–876. https://doi.org/10.1130/B30471.1.

Muller, C., 2018. Volumen de magma almacenado y eruptivo del volcán Turrialba. In: Memoria IV Congreso Nacional de Gestión del Riesgo y Adaptación al Cambio Climático, 10-11 de octubre, pp. 99–100. ISBN 978-9930-9684-0-6.

Murata, K.J., Dondoli, C., Saenz, R., 1966. The 1963–65 eruption of Irazú volcano, Costa Rica (the period of March 1963 to October 1964). Bull. Volcanol. 29, 763–793. https://doi.org/10.1007/BF02597194.

Oeser, M., Ruprecht, P., Weyer, S., 2018. Combined Fe-Mg chemical and isotopic zoning in olivine constraining magma mixing-to-eruption timescales for the continental arc volcano Irazú (Costa Rica) and Cr diffusion in olivine. Am. Mineral. 103 (4), 582–599. https://doi.org/10.2138/am-2018-6258.

Pagli, C., Wright, T.J., Ebinger, C.J., Yun, S.H., Cann, J.R., Barnie, T., Ayele, A., 2012. Shallow axial magma chamber at the slow-spreading Erta Ale Ridge. Nat. Geosci. 5, 284–288. https://doi.org/10.1038/ngeo1414.

Press, W.H., Teukolsky, S.A., Vetterling, W.T., Flannery, B.P., 2007. Numerical Recipes: The Art of Scientific Computing, 3rd ed. Cambridge Univ. Press, New York, p. 1235 (ISBN 0 521 43064 X).

Pritchard, M.E., Jay, J.A., Aron, F., Henderson, S.T., Lara, L.E., 2013. Subsidence at southern Andes volcanoes induced by the 2010 Maule, Chile earthquake. Nat. Geosci. 6, 632–636. https://doi.org/10.1038/ngeo1855.

Przeor, M., D'Auria, L., Pepe, S., Tizzani, P., Cabrera-Pérez, I., 2022. Elastic interaction between Mauna Loa and Kīlauea evidenced by independent component analysis. Sci. Rep. 12 (1), 1–13. https://doi.org/10.1038/s41598-022-24308-0.

Ramírez, R., Cordero, C., Alvarado, G.E., 2013. Variaciones y características en los cambios de nivel de la laguna cratérica del volcán Irazú (1965-2012), Costa Rica. Rev. Geol. Amér. Central 48, 141–157.

Reagan, M., Duarte, E., Soto, G.J., Fernández, E., 2006. The eruptive history of Turrialba volcano, Costa Rica, and potential hazards from future eruptions. In: Rose, W.I., Bluth, G.J.S., Carr, M.J., Ewert, J.W., Patino, L.C., Vallance, J.W. (Eds.), Volcanic Hazards in Central America: Geological Society of America Special Paper, 412, pp. 235–257. https://doi.org/10.1130/2006.2412(13).

Reagan, M.K., Gill, J.B., 1989. Coexisting calc-alkaline and high-niobium basalts from Turrialba Volcano, Costa Rica: Implications for residual titanates in arc magma sources. J. Geophys. Res. Solid Earth 94 (B4), 4619–4633. https://doi.org/10.1029/JB094iB04p04619.

Riedel, W., 1929. Zur Mechanik Geologischer Brucherscheinungen. Zentral-blatt fur Mineralogie, Geologie und Paleontologie B, pp. 354–368.

Rouwet, D., Mora-Amador, R., Ramirez, C., Gonzalez, G., Baldoni, E., Pecoraino, G., Inguaggiato, S., Capaccioni, B., Lucchi, F., Tranne, C.A., 2021. Response of a hydrothermal system to escalating phreatic unrest: the case of Turrialba and Irazú in Costa Rica (2007–2012). Earth Planets Space 73, 1–26. https://doi.org/10.1186/s40623-021-01471-8.

Ruprecht, P., Plank, T., 2013. Feeding andesitic eruption with a high-speed connection from the mantle. Nature 500, 68–72. https://doi.org/10.1038/nature12342.

Seropian, G., Kennedy, B.M., Walter, T.R., Ichihara, M., Jolly, A.D., 2021. A review framework of how earthquakes trigger volcanic eruptions. Nat. Commun. 12 (1), 1–13. https://doi.org/10.1038/s41467-021-21166-8.

Sigmundsson, F., Hreinsdóttir, S., Hooper, A., Arnadóttir, T., Pedersen, R., Roberts, M.J., Óskarsson, N., Auriac, A., Decriem, J., Einarsson, P., Geirsson, H., Hensch, M., Ófeigsson, B.G., Sturkel, E., Sveinbjörnsson, H., Feigl, K.L., 2010. Intrusion

triggering of the 2010 Eyjafjallajökull explosive eruption. Nature 468 (7322), 426–430. https://doi.org/10.1038/nature09558.
Tarasewicz, J., Brandsdóttir, B., White, R.S., Hensch, M., Thorbjarnardóttir, B., 2012. Using microearthquakes to track repeated magma intrusions beneath the Eyjafjallajökull stratovolcano, Iceland. J. Geophys. Res. Solid Earth 117 (B9). https://doi.org/10.1029/2011JB008751.
Vanicek, P., Castle, R.O., Balazs, E.I., 1980. Geodetic leveling and its applications. Rev. Geophys. 18 (2), 505–524. https://doi.org/10.1029/RG018i002p00505.
Williams, C.A., Wadge, G., 1998. The effects of topography on magma chamber deformation models: Application to Mt. Etna and radar interferometry. Geophys. Res. Lett. 25 (10), 1549–1552. https://doi.org/10.1029/98GL01136.
Wotzlaw, J.-F., Schaltegger, U., Frick, D.A., Dungan, M.A., Gerdes, A., Günther, D., 2013. Tracking the evolution of large-volume silicic magma reservoirs from assembly to super eruption. Geology 41, 867–870. https://doi.org/10.1130/G34366.1.
Xu, W., Jónsson, S., Corbi, F., Rivalta, E., 2016. Graben formation and dike arrest during the 2009 Harrat Lunayyir dike intrusion in Saudi Arabia: Insights from InSAR, stress calculations and analog experiments. J. Geophys. Res. Solid Earth 121 (4), 2837–2851. https://doi.org/10.1002/2015JB012505.